Novel rod-like carbon nanomaterials as NIR-responsive drug delivery system for potential anticancer applications

Mengru Liu[1], Xiaoxue Du[1], Jingyi Liu[1], Guangshuo Wang[1], Jiajia Yang[1], Xueling Wang[1], Shuai Han[1], and Zhongchao Huo[1]

[1]Hebei University of Engineering

November 9, 2023

Abstract

The combination of chemotherapy and photothermal therapy shows great potential to achieve synergistic anti-tumor effect. However, it is still a great challenge to design stimuli responsive drug release systems with integrated photothermal/chemotherapy functions. In this paper, novel rod-like carbon nanomaterials (RCNs) were prepared by soft template hydrothermal method with glucose as raw materials, which were proved to have good biocompatibility, excellent drug-loading capacity and high photothermal efficiency. After that, RCNs we used to load doxorubicin (DOX) for integrated photothermal/chemotherapy toward cancer, which demonstrated good treatment efficiency under NIR irradiation. Our approach provided a novel NIR-responsive nano platform for combined photothermal/chemotherapy toward cancer, which was considered to be of great potential in anticancer applications.

Novel rod-like carbon nanomaterials as NIR-responsive drug delivery system for potential anticancer applications

Mengru Liu[1,2], Xiaoxue Du[3], Jingyi Liu[3], Guangshuo Wang[3], Jiajia Yang[3], Xueling Wang[2], Shuai Han[3, *], Zhongchao Huo[2, *]

[1]College of Clinical Medicine, Hebei University of Engineering, Handan, P. R. China.

[2]Oncology Department No.1, Affiliated Hospital of Hebei University of Engineering, Handan, P. R. China.

[3]Handan Key Laboratory of Novel Nanobiomaterials, College of Materials Science and Engineering, Hebei University of Engineering, Handan, P. R. China.

Abstract

The combination of chemotherapy and photothermal therapy shows great potential to achieve synergistic anti-tumor effect. However, it is still a great challenge to design stimuli responsive drug release systems with integrated photothermal/chemotherapy functions. In this paper, novel rod-like carbon nanomaterials (RCNs) were prepared by soft template hydrothermal method with glucose as raw materials, which were proved to have good biocompatibility, excellent drug-loading capacity and high photothermal efficiency. After that, RCNs we used to load doxorubicin (DOX) for integrated photothermal/chemotherapy toward cancer, which demonstrated good treatment efficiency under NIR irradiation. Our approach provided a novel NIR-responsive nano platform for combined photothermal/chemotherapy toward cancer, which was considered to be of great potential in anticancer applications.

Keywords: carbon nanomaterials, photothermal performance, drug delivery, chemotherapy, synergistic therapies

Correspondence

Shuai Han, Handan Key Laboratory of Novel Nanobiomaterials, College of Materials Science and Engineering, Hebei University of Engineering, Handan, P. R. China.

Email: hanshuai@hebeu.edu.cn,

Zhongchao Huo, Oncology Department No.1, Affiliated Hospital of Hebei University of Engineering, Handan, P. R. China.

Email: huozhch@163.com

1 Introduction

Due to their serious metastasis and secondary infection, cancers have been the leading cause of human death. The general treatments of cancer include surgery[1, 2], chemotherapy[3, 4] and radiotherapy[5, 6], and so on. With the rapid development of nanotechnology and materials science, nano-drug delivery systems have caused more and more attention in the cancers' diagnosis[7] and treatment[8]. Among them, they include carbon nanomaterials[9-11], silica nanoparticles[12-14], gold nanoparticles[15-18] and so on. Among them, carbon nanomaterials have attracted extensive attention due to excellent water-solubility, high biocompatibility and low toxicity. It is worth to mention that nanoparticles below 200nm which have large specific surface area and drug loading capacity, could cause endocytosis and be taken up the cancer cells more easily, thus have a higher therapeutic efficiency. However, it is still a great challenge to prepare well-dispersed carbon nanoparticles ($<$ 200nm) with novel structures. On the other hand, glucose is considered to be an excellent raw material for preparing carbon nanomaterials, not only glucose is nontoxic and abundant bio-resource, but also it has been proved that the functional glycosylation groups retained on the surface of obtained carbon materials could help them to penetrate the cell membrane barrier more flexibly[19].

In recent years, stimuli responsive controlled nano-drug delivery systems have been proposed to improve the efficiency of treatment, such as temperature stimuli[20, 21], magnetism stimuli[22] and pH stimuli[23]. For example, Qi group developed a novel magnetic-targeted pH-responsive doxorubicin hydrochloride (DOX) carrier based on mesoporous $NiFe_2O_4$ nanospheres. The effective drug release amounts could increase more than 60% at pH 4.0 than that at neutral conditions within 48 h. Yang group prepared a novel multifunctional WS_2-IO@MS-PEG nanoscale platform [24]. Stimulated by NIR laser, the photothermal effect of WS_2 would trigger high efficiency release of DOX loaded in the platform, thereby lead to an increased killing efficiency for cancer cells. Darwin K. and his colleague synthesized chitosan - and nitrogen-doped graphene quantum dots with high drug carrying capacity and pH-controlled sustained drug release, which showed anticancer effects at the low concentration against lung cancer cell loading DOX[25]. At present, it is still a considerable challenge to obtain novel responsive nano-platforms with simple fabrication, good biocompatibility and high treatment efficiency.

In this paper, novel rod-like carbon nanomaterials (RCNs) were prepared by soft template hydrothermal method using glucose as raw materials. A series of characterizations were performed, which showed that the prepared carbon nanoparticles had excellent drug-loading capacity and high photothermal efficiency, in addition to good water solubility, stability and biocompatibility. After that, RCNs we used to load DOX for integrated photothermal/chemotherapy for cancer, which demonstrated good treatment efficiency. Our approach not only provided a new-typed carbon nano platform for drug delivery, but also supplied a new approach for practical cancer therapy in the future.

2 Experimental sections

2.1 Materials

Pluronic F127 ($EO_{106}PO_{70}EO_{106}$) was purchased from Sigma-Aldrich Co. Ltd. (U.S.A.). Concentrated sulfuric acid was purchased from Sinopharm Chemical Reagent Co. Ltd. (China). Doxorubicin, glucose and absolute alcohol were purchased from Aladdin Co. Ltd. (China). All chemicals were used as received without further purification.

2.2 Characterization

The microstructure and morphology of the prepared samples were observed by transmission electron microscopy (TEM, SU8220, Hitachi, Japan). The surface groups of RCNs and DOX@RCNs were characterized by FT-IR spectrometer (Spectrum 3, PerkinElmer, America). The absorbance was measured by UV-vis-NIR spectrophotometer (LAMBDA365, PerkinElmer, America). The specific surface area was measured by surface comparator (ASAP2460, Micromeritics, America). The temperature of the solutions was recorded by a thermal imaging camera (FLIR ONE Pro, Wilsonville, OR). Confocal microscopy photos were taken by an Olympus BX51 fluorescence microscope (Olympus, Tokyo, Japan).

2.3 Synthesis of RCNs

3.0g of F127 and 1.5g of glucose were dissolved in the 1.8M sulfuric acid solution, stirring for 10 h. Then, 30mL of the mixture was transferred to a 50mL Teflon-lined stainless steel autoclave for hydrothermal treatment for 30h at 140°C. After cooling to the room temperature, the products were collected by centrifugation and washed with water and ethanol several times. The obtained samples were dried at 60°C in vacuum oven overnight.

2.4 Synthesis of DOX@RCNs

200mg RCNs were dispersed into 50mL deionized water and treated with ultrasound for 20 min. After the ultrasonication, 40mg DOX was added to the above-mentioned dispersions stirred slowly overnight. Then, centrifugation was performed to eliminate the unadsorbed DOX. So far, DOX@RCNs were prepared. The drug loading rate was obtained by measuring the absorbance of the supernatant by UV-vis-NIR spectrophotometer. The adsorption capacity was calculated by the following formula:

$$q = \frac{(C_0 - C) \times V}{m} \tag{1}$$

q is the adsorption capacity of DOX sample, mg/g; C_0 is the initial concentration of DOX, mg/L; C is the concentration of DOX in the solution after adsorption, mg/L; V is the volume of solution, mL; m is the mass of adsorbent, g.

2.5 Photothermal Effects of RCNs and DOX@RCNs

Temperature changes were recorded during continuous NIR irradiation (808nm, 2.0w) to the solutions of RCNs at different concentrations (0, 25, 50, and 100μg/ml) for 600s. The temperature was recorded every 25s using a thermal imaging camera. To test the photothermal stability of the obtained RCNs, six cycles of heating and cooling for the solution were recorded. The photothermal conversion efficiency (η) of the RCNs solution was calculated according to the previous literature[26]. For the DOX@RCNs composites, temperature rise curve were firstly recorded during NIR irradiation (808nm, 2.5w) to the solutions of RCNs at 50μg/ml for 600s, then the temperature reduction curve was continued without NIR irradiation for another 700s.

2.6 Release of DOX for the DOX@RCNs under NIR irradiation

In brief, 10ml of DOX@RCNs aqueous solution (50μg/ml) was put in a dialysis bag (3,500Da), then soaked in a beaker containing 50mL PBS solution. The drug delivery experimental system was further put in the thermostat water bath (37), while the DOX@RCNs dialysis bag was adjusted to be irradiated by an 808nm laser (2.5W/cm^2). At a certain interval (20 min), 2mL of PBS buffer was removed from beaker for analysis, and an equal amount of PBS buffer at the same temperature was replenished. The release of DOX at each time point was measured by UV-vis-NIR spectrophotometer at the corresponding absorbance. The drug release experiment without laser irradiation was also performed using the similar methods as blank reference. The calculation formula is as follows:

$$Er = \frac{V_e \sum_1^{n-1} C_i + V_0 C_n}{m_{drug}} \quad (2)$$

E_r is the cumulative release of drugs; V_e is the replacement volume of PBS solution; V_0 is the total volume of the release medium; C_i is the concentration of the released liquid during each replacement sampling; m_{drug} is the total mass of the drug carried by the nanoparticles; n is the number of PBS replacement.

2.7 Cell Experiment

The cytotoxicity of RCNs and DOX@RCNs was assessed by MTT assay. MCF-7 cells were inoculated in plated in 96-well plates for 24h at the standard cell culture system. MCF-7 cells were treated with culture medium containing different concentrations (0-200μg/mL) of RCNs (or DOX@RCNs) for 24h. Subsequently, 20μL MTT was added to each well and incubated with the cells for 3h. After that, the liquid in each hole was sucked out and 150μL DMSO was added, then the value of each hole at the optimal absorbance (490nm) was measured and compared using a microplate reader. When evaluating the effect of PTT on cells, the MCF-7 cells were firstly inoculated for 24h, then the RCNs (or DOX@RCNs) was added incubated with irradiation with NIR light (808nm, 2.5W/cm^2) for 5 min, and the same method was used for measurement. In addition, in order to intuitively display the cell apoptosis promoted by nanomaterials, the experimental cells after 4 min irradiation were stained by DAPI and fluorescein-dUTP for 20 min, then taken photographs by confocal laser imaging systems.

3 Results and discussion

The novel RCNs were synthesized by soft-template hydrothermal method. As indicated in the TEM image (**Figure 1**), it was apparently demonstrated the products were constituted principally by rod-shaped carbon particles with relatively uniform dispersion and regular particle size. And the average size of the carbon rods was measured to be approximately 85-120nm in length, and 35-50nm in width. This novel morphology might be originated from the rodlike glucose-F127 monomicelles form, in which the polymerization, dehydration and nucleation of glucose took place, and finally form the rod-shaped nano structures.

The hydrodynamic diameter of RCNs was then measured by DLS. As shown in**Figure S1,** the size of the particles was calculated to be 110nm, which was consistent with the TEM results. Furthermore, the stability test of the RCNs was characterized by DLS over 2 weeks, as shown in**Figure S2** . It could be seen that the size exhibited almost negligible changes, which proved that the RCNs possess good stability in aqueous solution system.

The surface functional groups of carbon nanomaterials were further analyzed by FT-IR. **Figure 2** showed that the absorption peak at 3600-3200cm^{-1} was the stretching vibration of hydroxyl O-H, the absorption peak at 3000-2800cm^{-1} was the stretching vibration of saturated C-H, the absorption peak at 1770-1680cm^{-1} was the stretching vibration of ester carbonyl C=O, and the absorption peak at 1250-1000cm^{-1}was the stretching vibration of ester C-O.

The UV-vis-NIR spectra of the obtained RCNs in aqueous solution was shown in **Figure 3** , which revealed that the samples possessed high absorption in the NIR region around 650-900nm. The excellent NIR absorption characteristic of the samples encouraged us to explore their photothermal properties. The RCNs aqueous solution with different concentrations were irradiated under an 808nm laser at 2.5W/cm^2 power density. As shown in the**Figure 4** , under 808nm laser, the water temperature only increased by 3°C within 5 min. And it could be seen that the temperature of the RCNs solution increased more and more rapidly as the concentration increased. When the concentration was 50μg/mL, the temperature could raise to 45 in 5 min, while the concentration was 100μg/mL, it could raise to 54. The photothermal conversion efficiency of RCNs was calculated to be about 23.7 % using the reported literature. In the course of 6 cycles of photothermal heating and natural cooling **(Figure S3**), the photothermal heating effect did not change significantly, indicating that the RCNs had good photothermal stability.

In order to improve the therapeutic effect of the nanomaterials toward tumors, the nanocomposite with integrated thermo-chemotherapy performance was fabricated, while the classic DOX was used as the model anti-tumor drug. By the analysis of the DOX@RCNs, the drug loading rate of DOX for the nanocomposites was calculated to be 17.4%. The photothermal heating test was further arranged for the DOX@RCNs at the concentration of 50μg/mL. It could be seen in the **Figure 5** that the temperature could raise to 39 in 5 min, and 52 in 10 min, which showed excellent photothermal heating effect.

The drug release experiment under 808 nm laser radiation was explored, it could be seen from **Figure 6** that the release rate of DOX in the composites could achieve at 34.6% in 60 min, after 2h, the rates was calculated to be 64.7%. In the comparative experiments without irradiation, the corresponding releasing rates were calculated to be 5.7% and 7.2%, respectively. It could be concluded that infrared radiation can significantly increase the release of DOX, further realize integrated treatment of hyperthermia and chemotherapy.

Considering that low toxicity is a necessary condition for nano-drugs, the cell viability of MCF-7 cells incubated with different concentrations of RCNs and DOX@RCNs were conducted. The cell viability of MCF-7 cells incubated with two novel nano-drugs was shown in**Figure 7** . It could be observed that the carbon nanomaterials exhibit excellent biocompatibility, and have little cytotoxicity to MCF-7 cells up to a concentration of 300μg/mL. For comparison, the cytotoxicity for DOX@RCNs was slightly stronger. The cell survival rate decreased gradually with the increasing of the concentration of the sample, when the concentration was 300μg/mL, the cell survival rate was 78.6%.

Both the RCNs and DOX@RCNs were further explored their potential antitumor activity under NIR irradiation against MCF-7 cells. It could be seen that there was almost no cytotoxicity at the concentration of 50μg/mL for both RCNs and DOX@RCNs without NIR irradiation (**Figure 7**). In contrast, under NIR irradiation, two novel nano-drugs exhibited enhanced cytotoxicity against MCF-7 cells (**Figure S4**). It should be noted that no obvious cell apoptosis occurred after the MCF-7 cells were irradiated in the culture medium without the nanomaterials. The relative cell viabilities were calculated to be 50.2% at the RCNs concentration of 50μg/mL after 5 min of continuous irradiation ($2.5 W/cm^2$), suggesting the excellent photothermal toxicity effect of the RCNs. For the DOX@RCNs samples, benefiting from the effective NIR-sensitive release of DOX, DOX@RCNs exhibited stronger cytotoxicity than that of RCNs, while the relative cell viabilities decreased to 23.6% at the same test conditions.

In addition, confocal fluorescence microscopy was used to explore the toxicity effects of the nanomaterials (**Figure 8)** . DAPI, which could strongly bind to DNA, is a blue fluorescent dye used for fluorescence microscopy observation of living and fixed cells. In addition, fluorescein-dUTP is a green fluorescent dye which is used to label apoptotic cells. In this research, in order to display the cell apoptosis promoted by nanomaterials, DAPI/fluorescein-dUTP assays were performed to intuitively observe live and apoptotic cells. After 4 min irradiation, it could be seen that obvious apoptosis appeared in the MCF-7 cells for the RCNs group compared with the control ones, however, much more extensively apoptosis occurs for the DOX@RCNs group. This phenomenon was consistent with the MTT results.

4 Conclusions

In summary, novel rod-like carbon nanomaterials (RCNs) were prepared by soft template hydrothermal method with glucose as raw materials, which were proved to have good biocompatibility, excellent drug-loading capacity and high photothermal efficiency. Furthermore, DOX@RCNs were fabricated for integrated photothermal/chemotherapy toward cancer, which was proved to hold high photothermal efficiency, as well as excellent NIR-responsive DOX release properties. In vitro cell experiments indicated that the novel DOX@RCNs have good application prospects in the field of tumor therapy. This research provided a novel NIR-responsive nano platform for combined photothermal/chemotherapy toward cancer.

CONFLICT OF INTEREST

The authors declare no conflict of interest.

ACKNOWLEDGEMENTS

This work was supported by the foundation of Scientific research project of colleges and universities in Hebei Province (No. ZD2020126).

DATA AVAILABILITY STATEMENT

Author elects to not share data.

References

1. Toesca, A., Park, H.S., Ryu, J.M., Kim, Y.J., Lee, J., Sangalli, C.: Robot-assisted mastectomy: next major advance in breast cancer surgery. Brit. J. Surg.. 110(4), 502–503 (2023)
2. Jaron G. de Wit, et al.: EGFR-targeted fluorescence molecular imaging for intraoperative margin assessment in oral cancer patients: a phase II trial. Nat. Commun. 14, 4952 (2023)
3. Corti, C., et al.: Novel endocrine therapies: What is next in estrogen receptor positive, HER2 negative breast cancer?. Cancer Treat Rev.. 117, 102569 (2023)
4. Mouabbi, J. A., Singareeka Raghavendra, A., Bassett, R. L., Jr, Hassan, A., Tripathy, D., & Layman, R. M.: Survival Outcomes in Patients with Hormone Receptor-Positive Metastatic Breast Cancer with Low or No Erbb2 Expression Treated with Targeted Therapies Plus Endocrine Therapy. JAMA Netw. Open. 6(5), 2313017 (2023)
5. Song, Y.-C., et al.: Comparison of Supraclavicular Surgery Plus Radiotherapy Versus Radiotherapy Alone in Breast Cancer Patients with Synchronous Ipsilateral Supraclavicular Lymph Node Metastasis: A Multicenter Retrospective Study. Radiother Oncol.. 117(2), 208 (2023)
6. Reynolds, J.V., et al.: Trimodality Therapy Versus Perioperative Chemotherapy in the Management of Locally Advanced Adenocarcinoma of the Oesophagus and Oesophagogastric Junction (Neo-Aegis): An Open-Label, Randomised, Phase 3 Trial. Lancet Gasteroenterol. 8(11), 1015-1027 (2023)
7. Chen, Z., et al.: Dual-Responsive Triple-Synergistic Fe-Mof for Tumor Theranostics. ACS Nano. 17(10), 9003-9013 (2023)
8. Zhang, Y., et al.: Chiral Graphene Quantum Dots Enhanced Drug Loading into Small Extracellular Vesicles. ACS Nano. 17(11), 10191-10205 (2023)
9. Su, W., et al.: Targeted Degradation of Pd-L1 and Activation of the Sting Pathway by Carbon-Dot-Based Protacs for Cancer Immunotherapy, Angew. Chem. Int. Edit. 62(11), e202218128 (2023)
10. Jung, E., et al.: Tumor-Targeted Redox-Regulating and Antiangiogenic Phototherapeutics Nanoassemblies for Self-Boosting Phototherapy. Biomaterials. 298, 122127 (2023)
11. Yin, Y., et al.: Novel Combination Therapy for Triple-Negative Breast Cancer Based on an Intelligent Hollow Carbon Sphere. Research. 6, 0098 (2023)
12. He, L., Nan, X., Wang, T., and Bai, P.: Glutathione and Ph Serial Responsive Functional Mesoporous Silica Nanoparticles for Drug Delivery, MICRO NANO LETT, 15(5), 291-295 (2020)
13. He, Q., et al.: Near-Infrared-Activatable Protac Nanocages for Controllable Target Protein Degradation and on-Demand Antitumor Therapy. J. Med. Chem.. 66(15), 10458-10472 (2023)
14. Mao, Y., Zhang, Y., Wang, Y., Zhou, T., Ma, B., and Zhou, P.: A Multifunctional Nanocomposite Hydrogel with Controllable Release Behavior Enhances Bone Regeneration Regen Biomater. Regen. Biomater.. 28(10), rbad046 (2023)
15. Qu, X., et al.: Modulation of Intratumoral Fusobacterium Nucleatum to Enhance Sonodynamic Therapy for Colorectal Cancer with Reduced Phototoxic Skin Injury. ACS Nano. 17(12), 11466-11480 (2023)
16. Cai, L., et al.: Piezoelectric Metal-Organic Frameworks Based Sonosensitizer for Enhanced Nanozyme Catalytic and Sonodynamic Therapies. ACS Nano. 17(8), 7901-7910 (2023)
17. Xu, Y., et al.: A Smart "Energy Nanolock" Selectively Blocks Oral Cancer Energy Metabolism through Synergistic Inhibition of Exogenous Nutrient Supply and Endogenous Energy Production. Adv. Mater.. 35(3), 2207384 (2023)
18. Heravi, R.E., Zakeri, S., Nazari, P.: Anticancer Activity Evaluation of Green Synthesised Gold–Silver Alloy Nanoparticles on Colourectal Ht-29 and Prostate Du-145 Carcinoma Cell Lines. Micro Nano Lett.. 13(10), 1475-1479 (2018)

19. Yang, S., Chen, Z., Zhou, P., Xia, J., Deng, T., and Yu, C.: Carbon Dots Based on Endogenous Nutrients with Visible and Nir Fluorescence to Penetrate Blood-Brain Barrier. Carbon. 202, 130-140 (2023)
20. Zhang, T., Liu, N., Xie, C., and Xiao, X.: Self-Trigger and on-Demand Drug Delivery System Based on Tio2 Nanotube Arrays and Its Drug Release Behaviour. Micro Nano Lett.. 18(8), e12173 (2023)
21. Gui, X., et al.: Fluorescent Hollow Mesoporous Carbon Spheres for Drug Loading and Tumor Treatment through 980-Nm Laser and Microwave Co-Irradiation. Biomaterials. 248, 120009 (2020)
22. Oh, W.K., Yoon, H., and Jang, J.: Size Control of Magnetic Carbon Nanoparticles for Drug Delivery. Biomaterials. 31(6), 1342-1348 (2010)
23. Qi, Q., et al.: Investigation of Hollow Mesoporous Nife2o4 Nanospheres Fabricated Via a Template-Free Solvothermal Route as Ph-Responsive Drug Delivery System for Potential Anticancer Application. Cancer Nanotechnology. 14, 46 (2023)
24. Yang, G., Gong, H., Liu, T., Sun, X., Cheng, L., and Liu, Z.: Two-Dimensional Magnetic Ws2@Fe3o4 Nanocomposite with Mesoporous Silica Coating for Drug Delivery and Imaging-Guided Therapy of Cancer. Biomaterials. 60, 62-71 (2015)
25. Kurniawan, D., et al.: Plasma-Enabled Graphene Quantum Dot Hydrogels as Smart Anticancer Drug Nanocarriers. Small. 19 (20), 2206813 (2023)
26. Liu, J., et al.: Annular Mesoporous Carbonaceous Nanospheres from Biomass-Derived Building Units with Enhanced Biological Interactions. Chem. Mater.. 31(18), 7186–7191 (2019)
27. Liu Y, Ai K, Liu J, Deng M, He Y, Lu L: Dopamine-melanin colloidal nanospheres: an efficient near-infrared photothermal therapeutic agent for in vivo cancer therapy. Adv Mater.. 25(9), 1353-1359 (2013)

SUPPORTING INFORMATION

Additional supporting information may be found in the online version of the article at the publisher's website.

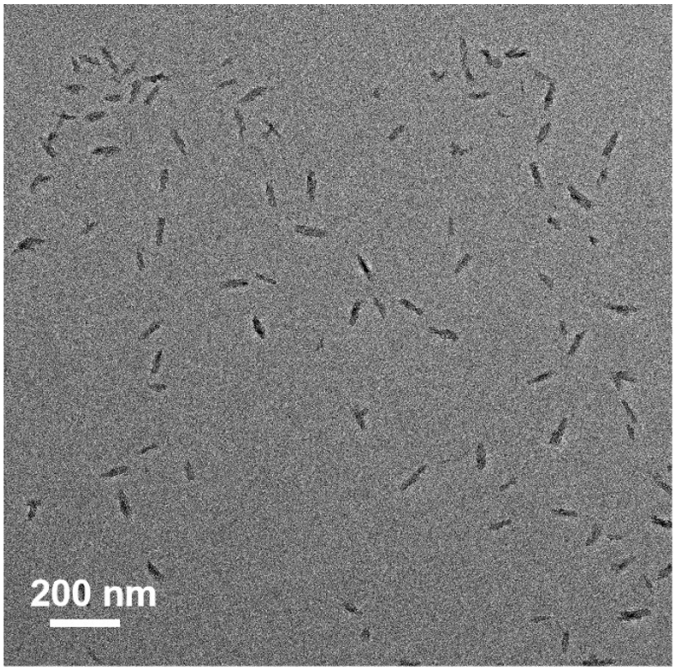

Figure 1 TEM images of obtained RCNs. The scale is 200nm.

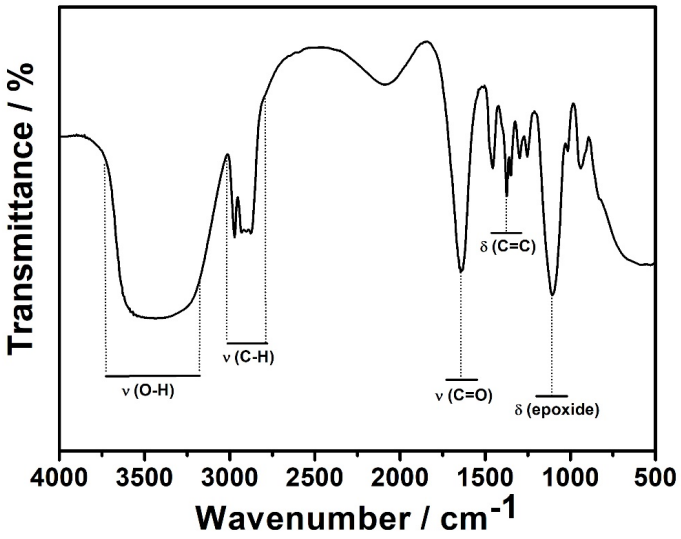

Figure 2 FITR spectrograms of RCNs. The wavenumber range is 4000-400cm^{-1}.

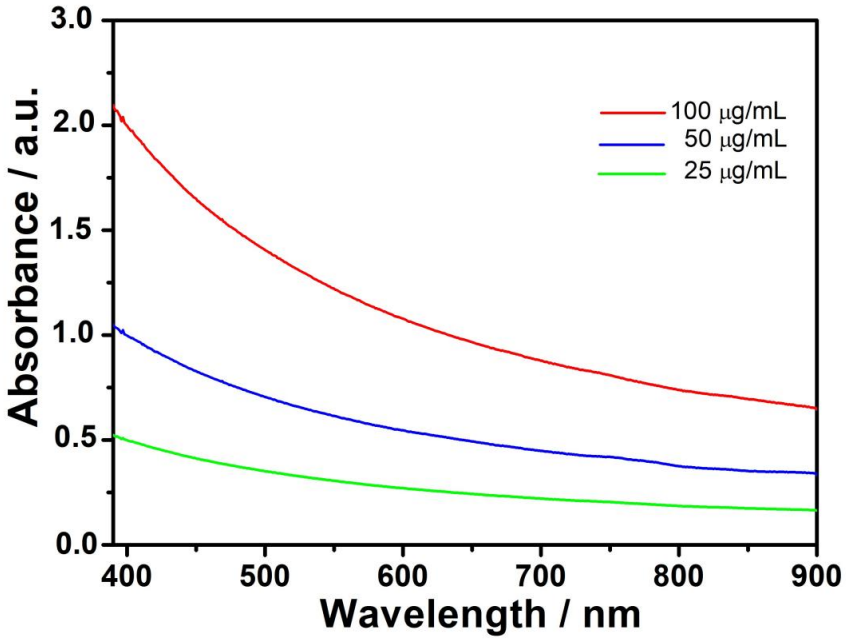

Figure 3 The UV-vis-NIR spectra of the obtained RCNs in aqueous solution at different concentrations.

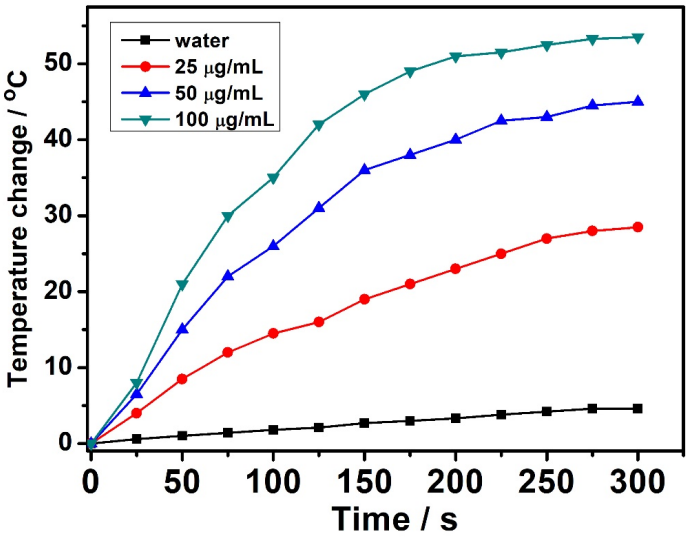

Figure 4 Temperature changes of different concentrations of RCNs aqueous solution with water as an empty control.

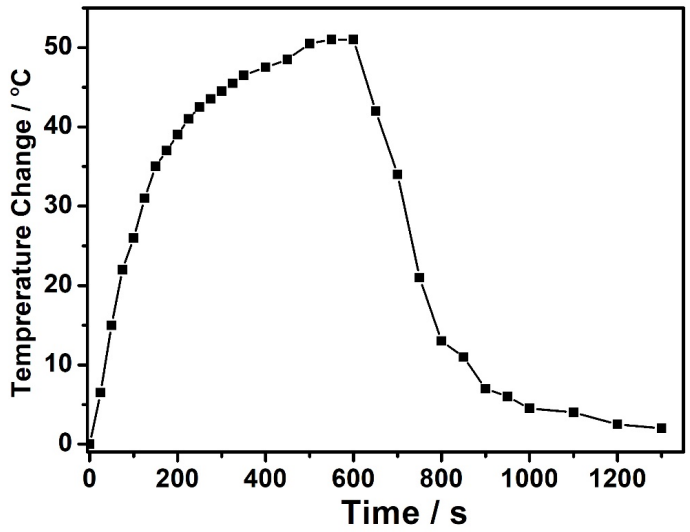

Figure 5 Temperature changes of 50μg/mL of RCNs aqueous solution within 20 min. The first 10 min is warming by 808nm laser at 2.5W/cm^2 power density, and the last is natural cooling.

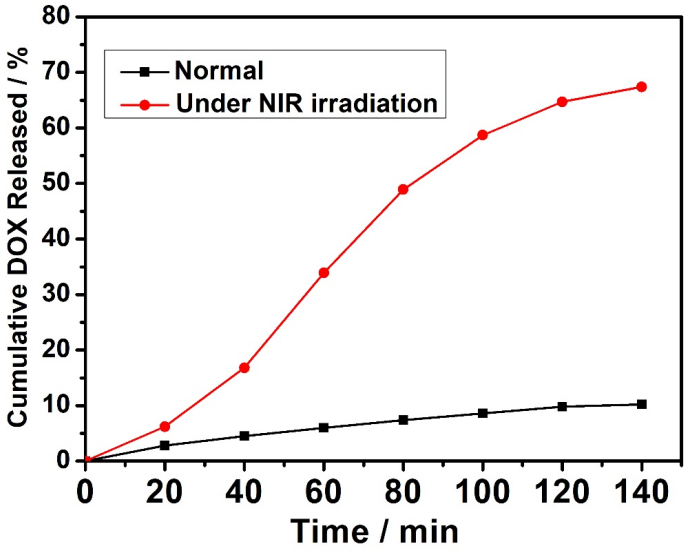

Figure 6 Cumulative release curves of DOX from DOX@RCNs at different situations.

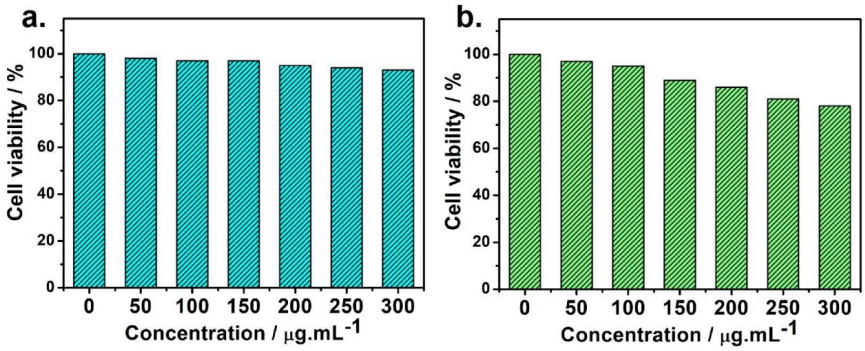

Figure 7 In vitro cytotoxicity of RCNs (a) and DOX@RCNs (b) on MCF-7 cells.

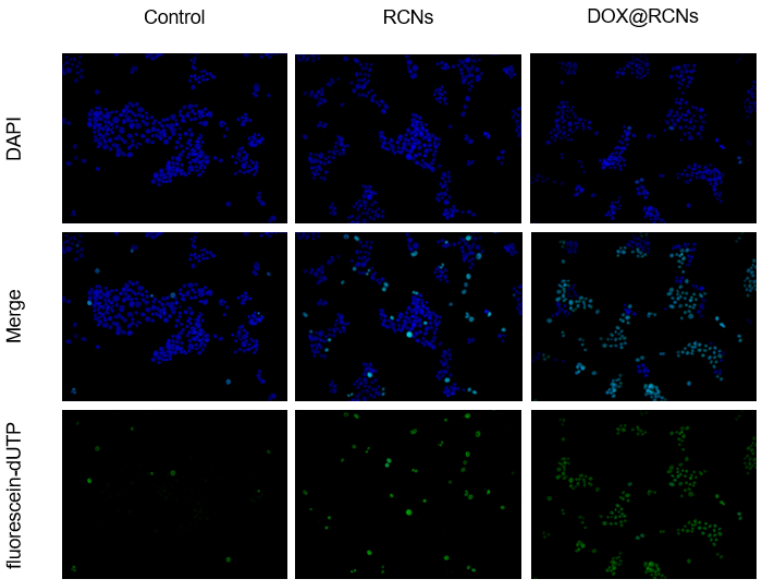

Figure 8 Schematic illustration and fluorescent photomicrographs of the MCF–7 cells after incubation with control group and RCNs and DOX@RCNs for 24h. Blue fluorescence indicates living and fixed cells, and green fluorescence indicates apoptotic cells.